Preparation and Mechanical Properties of Acrylonitrile-Butadiene-Styrene Copolymer/Clay Nanocomposites

Hun-Sik Kim, Byung Hyun Park, Jae Hoon Choi, Jin-San Yoon

Department of Polymer Science and Engineering, Inha University, Incheon 402-751, Korea

ABSTRACT: Bis(3-triethoxysilylpropyl) tetrasulfane (TSS) was reacted with the silanol groups of the commercially available clay, Closite®25A (C25A) to prepare TSS-C25A, which was melt-compounded with acrylonitrile-butadiene-styrene copolymer (ABS). The tetra sulfide groups of TSS-C25A may chemically react with the vinyl groups of ABS to enhance the interaction between the clay and ABS. The ABS/clay composites exhibited much higher tensile strength and elongation at break than the neat ABS. Especially the elongation at break of ABS/TSS-C25A composite was 5 times higher than that of neat ABS. The X-ray diffraction patterns of the clay showed that the d_{001} basal spacing was enlarged from 1.89 nm to 2.71–2.86 nm as a result of the compounding with ABS. According to the thermogravimetric analysis, the thermal decomposition of the composite took place at a slightly higher temperature than that of neat ABS. Intercalated/exfoliated coexisting structures were observed by transmission electron microscopy for the ABS/clay composites. © 2007 Wiley Periodicals, Inc. J Appl Polym Sci 107: 2539–2544, 2008

Key words: nanocomposites; acrylonitrile-butadiene-styrene copolymer (ABS); organoclay; mechanical properties

INTRODUCTION

Silane coupling agents are frequently employed to enhance rubber–filler interaction.[1–4] Proper selection of a silane coupling agent among the commercially available ones has become an important issue.[5]

Layered-silicate clays are very good nano-sized materials used as an effective reinforcing filler because of their high aspect ratio, platy morphology, and exceptionally stable oxide network.[6] In comparison to micron-scale fillers,[7] polymer/clay composites exhibit identical level of mechanical properties at much lower loading of the solid filler.

Many researches have been carried out to improve compatibility between the inorganic component and the polymer matrix because the properties of the composites depend strongly on the compatibility level.[8] The enhanced compatibility intercalate more easily the matrix polymer molecules between the clay layers and eventually facilitate the exfoliation and dispersion of the silicate layers in the polymer matrix.[9] The unique properties of polymer/clay composites come from the high degree of dispersion and the strong interaction between the clay layers and the polymer matrix.[8,10]

Introduction of functional groups, which are reactive toward the polymer matrix, to the clay surface favors higher degree of dispersion of the clay layers to achieve composites with advanced physical properties. However, little attention has been paid up to now to the composites composed of silicates having special functional groups.

Acrylonitrile-butadiene-styrene (ABS) resin is a widely used thermoplastic polymer. ABS consists of a two major phase system with grafted polybutadiene rubbery particles as the dispersed phase and poly(styrene-*co*-acrylonitrile) (SAN) matrix as the continuous phase. One of the morphological characteristics of ABS is that the rubbery particles are grafted by SAN. This enhances the interfacial bonding between the rubber particles and the SAN matrix and also facilitates the dispersion of the rubber particles in the matrix polymer. Since the properties of ABS are strongly influenced by the morphology and structure of the rubber phase, many efforts were devoted to controlling the rubber particle size[11] and the dispersion of the rubbery phase.[12]

In this study, bis(3-triethoxysilylpropyl)tetrasulfane (TSS) was reacted with silanol groups of a commercially available clay, Closite®25A (C25A) to prepare TSS-C25A. The tetra sulfide groups (TSS) may react with the vinyl groups of ABS to enhance the interaction between the TSS-modified clay and ABS. Morphology and mechanical properties of the ABS/TSS-C25A composites were compared to those of the corresponding reference clay composites.

EXPERIMENTAL

Materials

The clay used in this study was Cloisite®25A (C25A) (Southeastern Clay, USA). Acrylonitrile-butadiene-styrene copolymer (ABS) (RS-657) was obtained from LG Chemical (Korea). TSS was purchased from Shin-Etsu Chemical (Japan).

Clay modification with TSS

After TSS (4 g) was hydrolyzed for 2 h in a solution of hydrochloric acid in ethanol (90 wt %)/deionized water (10 wt %) mixture (400 g), the clay (20 g) was added and stirred at 70°C for 14 h. The resulting product was then filtered and repeatedly washed with ethanol at room temperature and dried in a vacuum oven at 60°C for at least 48 h and then ground to 53 μ-sized particles in a ball mill.

Blending of ABS/clay nanocomposites

ABS pellets and clay were melt-blended in a twin screw extruder (Twin Extruder BA-19 (L/D = 40) (Bautek, Korea)) at 220°C, 250 rpm for 5 min. The composites with various concentrations of C25A and TSS-C25A were prepared. Sheets of 350 μm thickness were made by melt pressing under a hot press (CARVER) at 220°C and 3 ton.

Polymer characterization

Fourier transformed infrared (FTIR) spectrum was recoded on a Perkin-Elmer Spectrum 2000 explore over a wave number range of 4000–400 cm.$^{-1}$

The variation of the interlayer distance of C25A in the nanocomposites was studied by means of wide angle X-ray scattering using a Rigaku DMAX 2500. The Cu Kα radiation source was operated at 18 kV. Patterns were recorded by monitoring those diffractions appeared in the 2θ range from 2° to 10° with a scanning rate of 1°/min.

Thermo-gravimetric analysis (TGA) was performed on a TGA-Q50 instrument (TA Instruments, DE) under a nitrogen flow at a heating rate of 20°C/min.

The tensile properties of the composites were measured with a universal testing machine (H 10KS, Hounsfield). Specimens were prepared according to ASTM D638. The cross-head speed was 10 mm/min. The results of 5 tests were averaged.

The morphological aspects of the composites have been examined by using transmission electron microscopy (TEM) to determine the internal micromorphology. JEOL-200 CX TEM, with an acceleration voltage of 200 kV, was used.

RESULTS AND DISCUSSION

Clay possesses net negative charge on its lamellar surface, and it can absorb cations, such as Na^+ or Ca^{2+}. Alkyl ammonium ions can replace the metal cations through the cation exchange process and occupy the gallery space between the nanoscaled layers of the clay[13] to alter the original silicate surface from being hydrophilic to organophilic. Because of the negative charge of the silicate layer, the cationic head group of an alkyl ammonium molecule preferentially resides at the layer surface with the aliphatic tails being removed from the surface.[14]

Many Si—OH groups still remain on the silicate surface even after the organophilic modification. Cloisite®25A (C25A) was treated with TSS to prepare TSS-C25A as shown in Scheme 1. Treatment of the silicate surface with the silane compound may raise the organophilicity, which would increase wetting of the clay layers with ABS. The tetrasufide functional groups, which are reactive toward the double bonds of ABS, may also enhance the interfacial interaction between the clay and ABS.

ABS and TSS-C25A are simultaneously introduced into a mechanical mixer such as two roll mill and internal mixer. During the melt mixing, the tetra sulfide groups of TSS-C25A will potentially react with the unsaturated double bonds of ABS as shown in Scheme 2.[15]

Figure 1 compares FTIR spectrum of C25A with that of TSS-C25A. The absorption bands at 2930 and
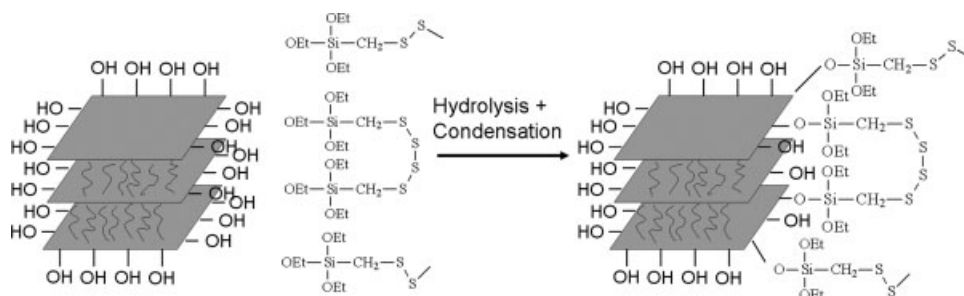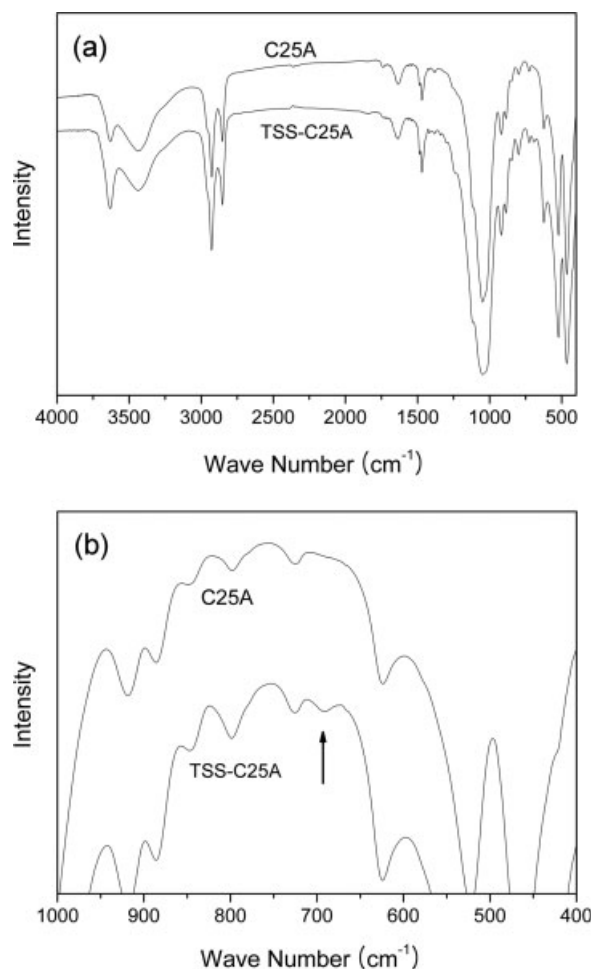
Scheme 1   Introduction of tetra sulfide groups to the clay surface.
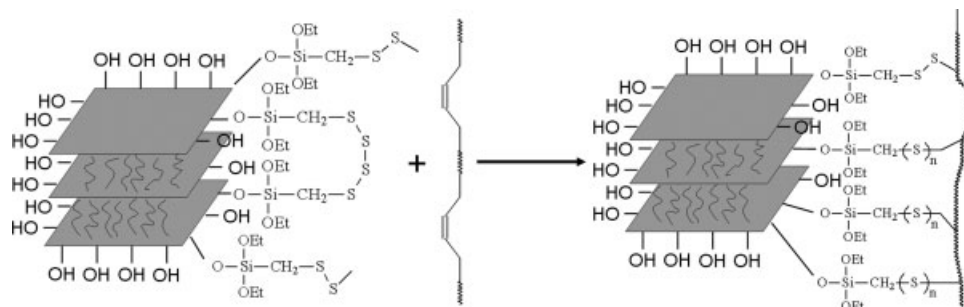
Scheme 2 Reaction of tetra sulfide groups of TSS-C25A with the vinyl groups of ABS.

2851 cm^{-1} were attributed to C—H stretching vibration.[11] The presence of two bands near 525 and 471 cm^{-1} came from Al(Mg)—O—Si stretching. The strong absorbance at 1087 cm^{-1} originated from Si—O—CH$_3$ stretching vibration.[16] The weak band at 797 cm^{-1} was assigned to Si—O—Si deformation. The tiny peak at 690 cm^{-1} corresponds to Si—C stretching indicative of the successful modification of C25A with TSS.

Figure 2 shows X-ray diffraction (XRD) patterns of TSS-C25A and C25A. TSS-C25A and pristine C25A exhibited almost the same interlayer distance. A possible explanation for the identical interlayer spacing of C25A and TSS-C25A is that, after the cation exchange reaction, the interlayer of the clay is filled with the organic molecules, which impede diffusion of the silane molecules to penetrate into the inter-space and react with the silanol groups inside between the clay sheets.[17] The silane molecules mainly reacted at the broken edges of the clay crystalline sheets where the silanol groups were more numerous than that on the plain surface of the clay sheets,[18–21] and the grafting reaction occurred mainly outside the interlayer of the clay.[22] A similar phenomenon has been reported by Herrera et al.[23]

ABS/Clay composites were prepared through melt intercalation process by using C25A and TSS-C25A. The intercalation of ABS chains enlarged the interlayer spacing relative to that of C25A, shifting the XRD peak toward a lower angle.

The XRD patterns of ABS/Clay composites are shown in Figure 3. Undoubtedly, the overall XRD patterns of the composites are essentially the same

Figure 1 FTIR spectra of C25A and TSS-C25A.
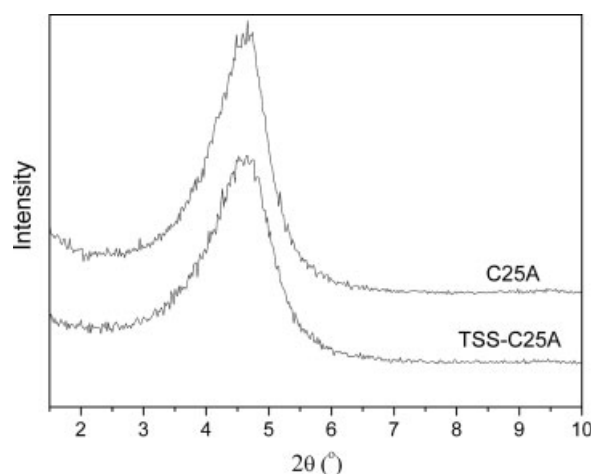
Figure 2 XRD patterns of C25A and TSS-C25A.
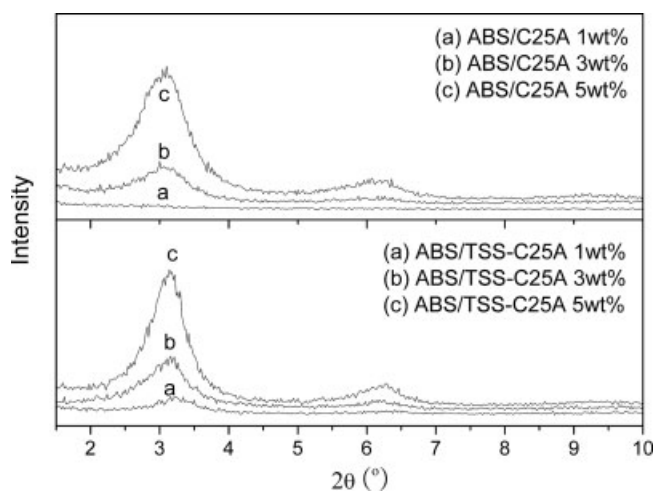
Figure 3 XRD patterns of ABS/C25A and ABS/TSS-C25A composites.

TABLE I
Interlayer Spacing of the Clays and ABS/Clay Composites

| Samples	d_{001} (nm)	2θ (°)
C25A	1.89	4.66
TSS-C25A	1.90	4.64
ABS/C25A (1 wt %)	–	–
ABS/C25A (3 wt %)	2.86	3.08
ABS/C25A (5 wt %)	2.84	3.10
ABS/TSS-C25A (1 wt %)	2.71	3.25
ABS/TSS-C25A (3 wt %)	2.80	3.15
ABS/TSS-C25A (5 wt %)	2.78	3.16

as those of C25A except the 001 reflection indicating that the overwhelming fraction of the composites retains the crystalline structure of the clay. However, the peak corresponding to d_{001}-spacing of ABS/ C25A composites appeared at lower 2θ angles than that of neat C25A indicative of the intercalation of ABS chains. According to the interlamellar distance calculated from the position of 001 reflection in Table I, the basal spacing of the composite was enlarged by 0.8–0.9 nm.

The 001 reflection peak of ABS/TSS-C25A composites appeared at almost the same position as that of ABS/C25A. Moreover the XRD peak of the former
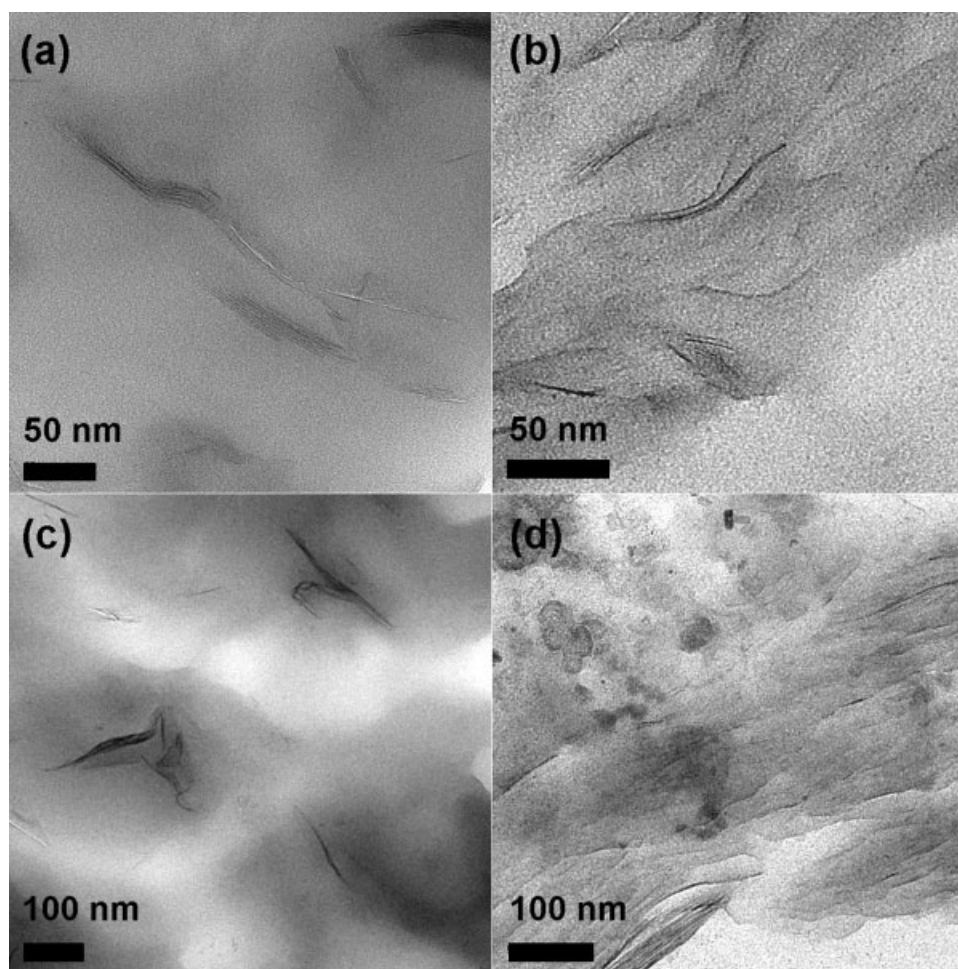
Figure 4 TEM micrograph of the composites (a), (c) ABS/C25A 3 wt %; (b), (d) ABS/TSS-C25A 3 wt %.
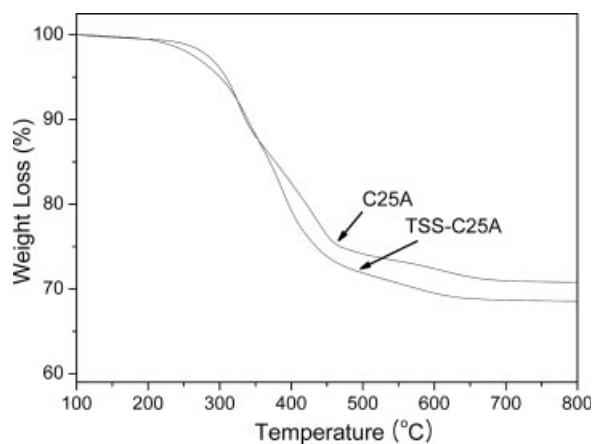
Figure 5 TGA plots of C25A and TSS-C25A.

Figure 6 TGA plots of ABS and the ABS/clay composites.

composite was more intense than that of the latter. This is contrary to the expectation, because partial disruption of parallel stacking of the clay layers coming from the enhanced interfacial interaction between TSS-C25A and ABS due to the plausible chemical reaction and the increased wetting was expected to attenuate the XRD peak.[24]

Morphology of the composites was examined using TEM to observe the dispersion state of the silicate layers. The TEM micrographs in Figure 4 demonstrate that 1–2 nm sized silicate layers are arranged in good order and are well dispersed in ABS/C25A as well as in ABS/TSS-C25A composites. No clear indication of full exfoliation of the clay layers can be observed in both the two composites.

Figure 5 represents TGA thermograms of C25A and TSS-C25A measured under nitrogen atmosphere. After the modification with TSS, the clays were Soxhlet extracted with chloroform for a week to remove unbound TSS and dried in a vacuum oven to a constant weight. The weight loss of TSS-C25A (31.4 wt %) was higher than that of C25A (29.1 wt %). The difference in the weight loss came from the additional weight decrease due to the grafted TSS for sure.

Thermogravimetric analyses of the composites are shown in Figure 6. It can be seen that the onset temperature of thermal degradation of ABS went up slightly as a result of compounding with the clay. Such enhanced thermal stability has already been
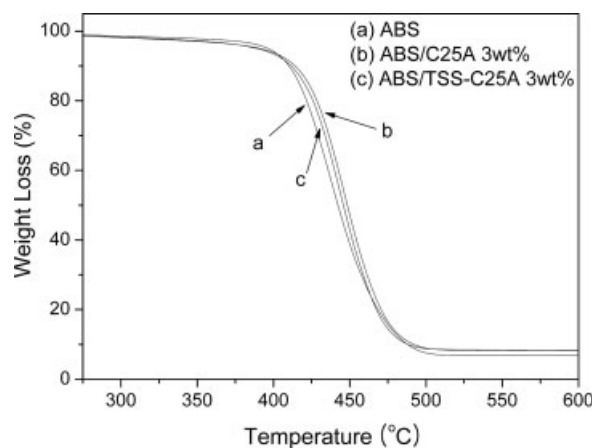
reported for other composites with silicate layers based on matrices such as nylon-6,[25] polystyrene,[26] or PC/ABS.[27] The improvement of thermal stability of the composites is attributed to the shielding effect of the clay layers. Since the layers of organo-modified silicate are impermeable to small molecules generated during the thermal degradation process, the degradation products have to take a long way around the clay layers.[28] Thus, the addition of organoclay to polymer matrix should slow down the release rate of the decomposed products to endow the degradation products more chance to bind back to the undecomposed residual polymer matrix. This presumption is plausible because reactive radicals are usually formed during the thermal degradation of the matrix polymers.

Tensile strength and elongation of ABS/Clay composites are summarized in Table II. Both the tensile strength and elongation at break of ABS increased as a result of compounding with the clays whether the clays had been modified with TSS or not. The clays acted as reinforcing filler because of their high aspect ratio and platelet structure to increase the tensile strength values. It is to be noted here that incorporation of the TSS modified clays improved the tensile strength and elongation at break of ABS more significantly than that of C25A. ABS/TSS-C25A composite with 3 wt % of TSS-C25A exhibited elongation at break almost 5 times higher than neat ABS. Tensile strength of ABS/TSS-C25A was 40% higher than

TABLE II
Tensile Properties of Neat ABS and ABS/Clay Composites

Samples	Tensile strength (MPa)	Young's modulus (MPa)	Elongation at break (%)
ABS	31.96 ± 0.95	3108 ± 178	4.65 ± 0.89
ABS/C25A (3 wt %)	35.62 ± 1.13	2956 ± 254	5.29 ± 1.17
ABS/C25A (5 wt %)	39.37 ± 1.31	2982 ± 169	4.60 ± 0.84
ABS/TSS-C25A (3 wt %)	43.20 ± 0.80	3386 ± 260	14. 81 ± 1.73
ABS/TSS-C25A (5 wt %)	42.64 ± 1.24	2852 ± 249	22.82 ± 2.07

that of neat ABS. The improved tensile properties of ABS/TSS-C25A composites compared to those of neat ABS and ABS/C25A composites came from the enhanced interfacial interaction because of the chemical reaction between the tetra sulfide groups of TSS-C25A and the unsaturated bonds of ABS.

References

1. Castellanoa, M.; Conzattia, L.; Costab, G.; Falquib, L.; Tartarroa, A.; Valentia, B.; Negroni, F. Polymer 2005, 46, 695.
2. López-Manchado, M. A.; Herrero, B.; Arroyo, M. Polym Int 2004, 53, 1766.
3. Ganter, M.; Gronski, W.; Reichert, P.; Mulhaupt, R. Rubber Chem Technol 2001, 74, 221.
4. Garde, K.; McGill, W. J.; Woolard, C. D. Plast Rubber Compos 1999, 28, 1.
5. Poh, B. T.; Ng, C. C. Eur Polym J 1998, 24, 975.
6. Pinnavaia, T. J. Science 1983, 220, 365.
7. Wang, Y. M. Organosil Mater Appl Chin 1992, 5, 11.
8. Giannelis, E. P. Adv Mater 1996, 8, 29.
9. Wang, S.; Li, Q.; Qi, Z. Key Eng Mater 1998, 137, 87.
10. Krikorian, V.; Pochan, D. J Chem Mater 2003, 15, 4317.
11. Donald, A. M.; Kramer, E. J. J Appl Polym Sci 1982, 27, 3729.
12. Bucknall, C. B.; Cote, F. F. P.; Partridge, I. K. J Mater Sci 1986, 21, 301.
13. Burnside, S. D.; Giannelis, E. P. Chem Mater 1995, 7, 1597.
14. Chen, G. X.; Yoon, J. S. Polym Int 2005, 54, 939.
15. Brinke, J. W. X; Debnath, S. C.; Reuvekamp, L. A. E. M.; Noordermeer, J. W. M. Compos Sci Technol 2003, 63, 1165.
16. LeBaron, P. C.; Pinnavaia, T. J. Chem Mater 2001, 13, 3760.
17. Chen, G. X.; Choi, J. B.; Yoon J. S. Macromolecules 2005, 26, 183.
18. Chen, G. X.; Choi, J. B.; Yoon, J. S. Macromol Rapid Commun 2005, 26, 183.
19. Pinnavaia, T. J.; Beall, G. W. Polymer-Clay Nanocomposites; Wiley: New York, 2000.
20. Theng, B. K. G. Chemistry of Clay-Organic Reactions; Wiley: New York, 1974.
21. Ray, S. S.; Okamoto, K.; Okamoto, M. Macromolecules 2003, 36, 2355.
22. Fujii, K.; Hayashi, S.; Kodama, H. Chem Mater 2003, 15, 1189.
23. Herrera, N. N.; Letoffe, J. M.; Putaux, J. L.; David, L.; Bourgeat-Lami, E. Langmuir 2004, 20, 1564.
24. Chen, G. X.; Yoon J. S. Polym Degrad Stabil 2005, 88, 206.
25. Pramoda, K. P.; Liu, T.; Liu, Z.; He, C.; Sue, H. J. Polym Degrad Stabil 2003, 81, 47.
26. Zhu, J.; Wilkie, C. A. Polym Int 2000, 44, 1158.
27. Zong, R.; Hu, Y.; Wang, S.; Song, L. Polym Degrad Stabil 2004, 83, 423.
28. Zanetti, M.; Camino, G.; Mulhaupt, R. Polym Degrad Stabil 2001, 74, 413.